This full text paper was peer reviewed at the direction of IEEE Communications Society subject matter experts for publication in the IEEE INFOCOM 2010 proceedings
This paper was presented as part of the main Technical Program at IEEE INFOCOM 2010.

Minimizing Energy Consumption with Probabilistic Distance Models in Wireless Sensor Networks

Yanyan Zhuang Jianping Pan Lin Cai
University of Victoria, Victoria, BC, Canada

***Abstract*—Minimizing energy consumption in wireless sensor networks has been a challenging issue, and grid-based clustering and routing schemes have attracted a lot of attention due to their simplicity and feasibility. Thus how to determine the *optimal grid size* in order to minimize energy consumption and prolong network lifetime becomes an important problem during the network planning and dimensioning phase. So far most existing work uses the average distances within a grid and between neighbor grids to calculate the average energy consumption, which we found largely underestimates the real value. In this paper, we propose, analyze and evaluate the energy consumption models in wireless sensor networks with probabilistic distance distributions. These models have been validated by numerical and simulation results, which shows that they can be used to optimize grid size and minimize energy consumption accurately. We also use these models to study variable-size grids, which can further improve the energy efficiency by balancing the relayed traffic in wireless sensor networks.**

***Index Terms*—Wireless sensor networks, grid-based clustering, distance distribution, energy consumption**

I. Introduction

Recent advances in computer, communication and manufacturing technologies have made the miniaturization of wireless sensor nodes possible and viable for large-volume commercial production as well as large-scale real-world deployment. In typical wireless sensor network applications, sensor nodes are deployed in the sensing field and left unattended to continuously monitor and report environment events and parameters. To ensure reliability, low-cost sensor nodes are usually deployed densely in the field; on the other hand, redundant sensor nodes can stay in the sleep mode to conserve energy, since in many cases it is very difficult, if not impossible, to replace the energy supply on the sensor nodes that are already deployed. Energy conservation is also very important for nodes even with energy harvesting capabilities.

Since wireless communication is a major source of energy consumption in sensor networks, many research efforts have appeared in the literature to improve the energy efficiency of wireless sensor networks, covering almost all aspects of the communication stack [1], [2]. Among them, grid-based clustering and routing schemes, in which clusters are equal-sized square grids in a two-dimensional plane, have attracted a lot of attention due to their simplicity and feasibility, especially with GPS and other localization techniques. Once the grid structure is established, nodes can communicate locally with their grid head, and reach the data processing center, or the sink node, through neighbor grids.

Thus in grid-based clustering schemes, an important problem is to determine the optimal grid size in order to minimize energy consumption and prolong network lifetime, since the grid structure will dominate the communication distance between sensor nodes. Various griding schemes have been proposed, but so far most existing work has used the average distance within a grid or between neighbor grids to calculate the energy consumption. However, we found that the average distance approach is not accurate and can largely underestimate the real value due to the superlinear path loss exponent of over-the-air wireless transmissions.

In this paper, we propose, analyze and evaluate the energy consumption models that are not relying on the average distance calculation, but using the probabilistic distance distributions for different sensor node locations. We are aiming at finding the *optimal grid size* by using these more accurate models, instead of proposing new efficient routing schemes, which is out of the scope of this paper. Although these models have higher computation complexity than those using the average distance, they are validated by our numerical and simulation results. We have also confirmed that it is important and worthwhile to pay the extra effort: the optimal grid size and the minimal energy consumption are both very different from those simply using the average distance.

The contributions of this paper are threefold. First, to the best of our knowledge, this is the first time that the energy consumption in wireless sensor networks is captured with models using probabilistic distance distributions, which was considered very difficult previously. Second, we also illustrate how to use these models in a computation-effective manner with polynomial fitting, through which it is still possible to optimize grid size and minimize energy consumption accurately. Third, we use these models to illustrate how to further improve the energy efficiency in wireless sensor networks by using variable-size grids, which has only been approached in the literature in one-dimensional or quasi-two-dimensional cases.

The remainder of this paper is structured as follows. In Section II, we briefly overview the grid-based clustering and routing schemes and compare with the most related work. In Section III, we present the energy consumption models with probabilistic distance distributions for grid-based wireless sensor networks, followed by numerical and simulation results in Section IV. We use these models to further improve the energy efficiency in wireless sensor networks with variable-size grids in Section V, followed by further discussion and concluding remarks in Section VI.

978-1-4244-5837-0/10/$26.00 ©2010 IEEE

This full text paper was peer reviewed at the direction of IEEE Communications Society subject matter experts for publication in the IEEE INFOCOM 2010 proceedings
This paper was presented as part of the main Technical Program at IEEE INFOCOM 2010.

II. Background and Related Work

In large-scale wireless sensor networks, an efficient organization of network topology is very important to minimize energy consumption and prolong network lifetime. Clustering has been an effective way of organizing sensor networks; grid-based clustering in particular due to its simplicity has a good potential in efficient topology control.

A. Clustering Schemes

In clustering schemes, sensor nodes are partitioned into a number of small clusters. Each cluster has a coordinator, the cluster head (CH), and a number of cluster nodes. Clustering results in a two-tier hierarchical structure, in which cluster nodes transmit data to their own CH directly, while CHs collect the data and send them to the sink node through the CHs in other clusters. Meanwhile, redundant cluster nodes can be put into the sleep mode, since sensors within the sense and transmission range of others have no need to be active all the time. Therefore, clustering schemes are widely used in wireless sensor networks, not only due to their simple node coordination, but also because they use multi-hop routing between CHs to avoid long-range transmissions.

Many clustering schemes have been proposed in various contexts. For example, Choi et al. propose a Two-Phase Clustering (TPC) scheme [6], which includes a cluster head electing stage and an energy-saving data relay link setup. Mhatre et al. determined the optimal node density by using Voronoi cells to guarantee a lower bound of network lifetime [11]. Younis et al. proposed a Hybrid Energy-Efficient Distributed (HEED) clustering scheme [12], introducing a variable known as cluster radius, which defines the transmission power to be used for intra-cluster broadcast. These clustering schemes are heuristic in nature, and need time synchronization or frequent message exchanges between sensor nodes.

However, one general simplification in sensor network analysis is the use of the average distance in calculating energy consumption [15] [16], including our previous work [4]. As simple as they might be, the average distance models can largely underestimate the distance distribution between sensor nodes, and the gap between the actual energy consumption and that by the average distance models will become even larger because of the superlinear path loss exponent.

B. Grid-based Clustering

Among all the existing clustering techniques, grid-based clustering, which partitions the network into equal-sized square grids, has a simple structure with less management overhead, and all nodes in one grid are equivalent from the routing perspective. With the assistance of GPS or localization techniques [13], the square grid also provides an easier coordination among all sensor nodes in the network. Thus, it allows for a theoretical analysis while still being useful enough to incorporate all the important elements of a network.

Grid-based clustering also greatly facilitates the data dissemination process, so that once the sensor nodes have sensed data, they can transmit without the need of setting up a routing path explicitly. This way, data can be propagated quickly without any extra overhead of route construction or maintenance, which is desirable for real-time applications.

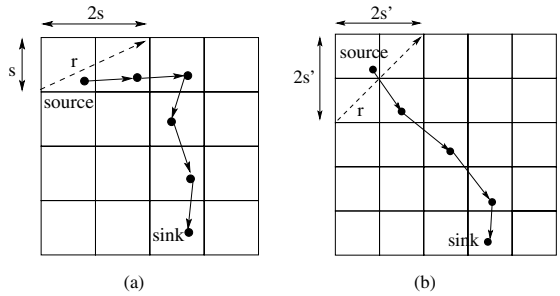

Fig. 1. Manhattan Walk and Diagonal-First Routing.

In [4] we examined two routing schemes, Diagonal-First routing and Manhattan Walk, which only rely on the one-hop geographical information. A cluster in these two schemes is a square region in which any node can communicate via a single-hop transmission with any other nodes in a neighbor cluster. Thus only one representative node in each cluster needs to be active in the routing process at any given time. In Manhattan Walk as shown in Fig. 1(a), the grid size s is chosen such that any two nodes in horizontally or vertically adjacent grids are within the maximum transmission range (r) of each other, i.e., $s \leq r/\sqrt{5}$. This is similar to GAF [14]. Diagonal-First routing uses a smaller grid size to divide the network, i.e., $s' \leq r/\sqrt{8}$, allowing nodes in diagonal grids to be in the same transmission range as well, as shown in Fig. 1(b). Given the same maximum transmission range and source-sink locations, Diagonal-First Routing will have a smaller or equal number of hops compared to Manhattan Walk. In this paper we will continue using these two routing schemes and analyze their performance with distance distributions.

C. Variable-size Clustering

The unique many-to-one data forwarding pattern in sensor networks makes the traffic volume highly skewed: the closer a node is to the sink, the more traffic it has to relay. These close-to-sink nodes become the bottleneck in the network and will consume their energy much faster than other nodes, which leads to an earlier "breakdown" of the network.

There have been some recent efforts in the design and analysis of nonuniform clustering schemes. EECS [18] introduces a distance-based cluster formation, where clusters farther away from the sink have smaller sizes, so the energy could be preserved for long-haul data transmission to the sink. However, this model does not consider multi-hop networks, where a single long-range transmission can be replaced by multiple relayed ones. [17] proposed an unequal clustering model to balance the energy consumption in multi-hop networks, where CHs are deterministically deployed at precomputed locations. [8] studied a simple linear network and deduced the relationship between the optimal radio range and traffic load distribution in one-dimensional networks. For nonlinear networks, the problem becomes more complicated. While [10]

This full text paper was peer reviewed at the direction of IEEE Communications Society subject matter experts for publication in the IEEE INFOCOM 2010 proceedings
This paper was presented as part of the main Technical Program at IEEE INFOCOM 2010.

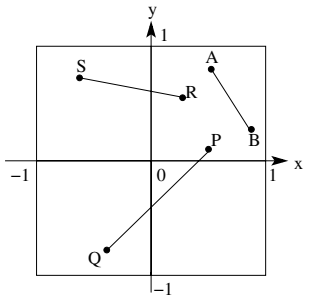

Fig. 2. Random Points in Unit Grids.

proposed variable grid sizes in two-dimensional networks, they only partition the network according to the traffic pattern in one dimension and left the other dimension intact, i.e., quasi-two-dimensional. The work in [19] divides the sensors into clusters according to the hop count from the sink, and the size of the clusters grows with the distance increase in a power-of-2 function without optimizing the size ratio.

In this paper, we are inspired by the variable-size griding in image processing [20], and we use the technique to further improve the energy efficiency by balancing the traffic volume in grid-based clustering schemes. The simulation results show the promising potentials of this technique.

III. Distance Distribution Models

Energy consumption is an important performance metric for wireless sensor networks, and in many cases the major source of it is wireless transmission, which largely depends on the distance between transceivers. In this section we derive probabilistic distance distributions and polynomial fitting to model random sensor networks, by using the geometric properties of grid-based clustering. The models facilitate distance calculation and can yield results with high accuracy. To the best of our knowledge, no comparable efforts in wireless sensor networks have used this approach to characterize random node distribution and calculate energy consumption accordingly.

A. Coordinate Distributions

Given two nodes on the plane with coordinates (X_1, Y_1) and (X_2, Y_2), their distance $D = \sqrt{(X_1 - X_2)^2 + (Y_1 - Y_2)^2}$. Thus, the geometric distribution of node distance, $P(D \leq d)$, is determined by the distribution of these coordinates.

With a grid-based clustering scheme, there are three possible cases of transceiver locations for a wireless transmission: between a cluster node and the grid head within the same grid; between two grid heads of neighbor grids, where the grids can be diagonal or parallel to each other. Thus, the coordinate distributions of these nodes will belong to one of the three cases shown in Fig. 2 and detailed as follows.

1) Two Random Nodes in the Same Grid: For nodes A and B in Fig. 2, they are uniformly distributed within the same grid, where one of them is a cluster node and the other one is the grid head. With the coordination system shown in the figure, the coordinate distributions of A and B are

$$f_{X_1}(x) = f_{X_2} = f_{Y_1} = f_{Y_2} = H(x) - H(x-1), \quad (1)$$

where $H(x)$ is the Heaviside Step Function[1] [21] defined as

$$H(x) = \begin{cases} 0 & x < 0 \\ 1 & x \geq 0 \end{cases}, \quad (2)$$

i.e., $X_1, X_2, Y_1, Y_2 \sim U[0, 1]$.

2) Two Random Nodes in Diagonal Neighbor Grids: Following the same notation, when nodes P and Q are in two diagonal neighbor grids, their coordinate distributions are

$$\begin{cases} f_{X_1}(x) = f_{Y_1}(x) = H(x) - H(x-1) \\ f_{X_2}(x) = f_{Y_2}(x) = H(x+1) - H(x) \end{cases}, \quad (3)$$

i.e., $X_1, Y_1 \sim U[0, 1]$ and $X_2, Y_2 \sim U[-1, 0]$.

3) Two Random Nodes in Parallel Neighbor Grids: Similarly, for nodes R and S in two parallel neighbor grids, their coordinate distributions are

$$\begin{cases} f_{X_1}(x) = f_{Y_1}(x) = f_{Y_2}(x) = H(x) - H(x-1) \\ f_{X_2}(x) = H(x+1) - H(x) \end{cases}, \quad (4)$$

i.e., $X_1, Y_1, Y_2 \sim U[0, 1]$ and $X_2 \sim U[-1, 0]$.

Although we use unit square grids here, it should be noted that such a formulation is flexible enough to be extended to non-square rectangles, as well as neighbor grids of different sizes, which will be shown in Section V. The same approach can be applied to non-square sensing fields as well, although the computation may become more involved.

B. Distance Distributions

Once the coordinate distributions of two nodes are obtained, we can get the distance distribution according to its definition. Without loss of generality, let $V = X_1 - X_2$ (or $Y_1 - Y_2$), $S = V^2$, $Z = S_X + S_Y$ and $D = \sqrt{Z}$, and our goal is to obtain $f_D(d)$, i.e., the distance probability density function of two nodes for the three cases described above.

1) Difference Distribution: With $V = X_1 - X_2$, the cumulative distribution function of V is therefore $F_V(v) = P(X_1 - X_2 \leq v) = \int_{x_1 - v}^{\infty} \left[\int_{-\infty}^{\infty} f_{X_1, X_2}(x_1, x_2) dx_1 \right] dx_2 = \int_{-\infty}^{v} \left[\int_{-\infty}^{\infty} f_{X_1, X_2}(x, x - v) dx \right] dv$, where $f_{X_1, X_2}(x_1, x_2)$ is the joint probability density function of X_1 and X_2. Since X_1 and X_2 are independent, $F_V(v) = \int_{-\infty}^{v} \left[\int_{-\infty}^{\infty} f_{X_1}(x) f_{X_2}(x - v) dx \right] dv$. Denote the probability density function by $f_V(v)$, we have

$$f_V(v) = \int_{-\infty}^{\infty} f_{X_1}(x) f_{X_2}(x - v) dx. \quad (5)$$

2) Square Distribution: With $S = V^2$, $F_S(s) = P(V^2 \leq s) = P(-\sqrt{s} \leq V \leq \sqrt{s}) = \int_{-\sqrt{s}}^{\sqrt{s}} f_V(v) dv = F_V(\sqrt{s}) - F_V(-\sqrt{s})$, then we have

$$f_S(s) = F'_S(s) = \frac{f_V(\sqrt{s}) + f_V(-\sqrt{s})}{2\sqrt{s}}. \quad (6)$$

[1]Here we assume $H(x) \equiv H_1(x)$ for notation convenience.

This full text paper was peer reviewed at the direction of IEEE Communications Society subject matter experts for publication in the IEEE INFOCOM 2010 proceedings
This paper was presented as part of the main Technical Program at IEEE INFOCOM 2010.

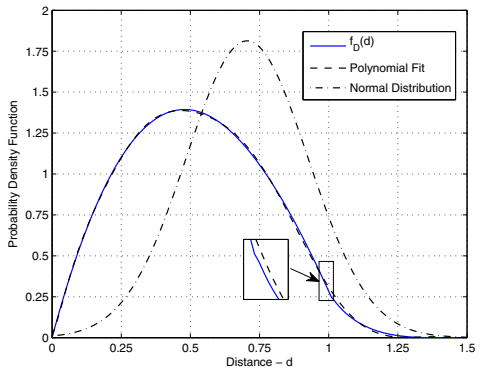

Fig. 3. Distance Distribution within a Unit Square.

3) Sum Distribution: With $Z = S_X + S_Y$, following the same approach in Section III-B1, $F_Z(z) = P(S_X + S_Y \leq z) = \int_{-\infty}^{z} \left[\int_{-\infty}^{\infty} f_{S_X,S_Y}(x, z-x)dx\right] dz$. Thus the following convolution notation is used to obtain $f_Z(z)$:

$$f_Z(z) = \int_{-\infty}^{\infty} f_{S_X}(x) f_{S_Y}(z-x)dx. \tag{7}$$

4) Square-Root Distribution: With $D = \sqrt{Z}$, the distance distribution $f_D(d)$ can be derived by

$$f_D(d) = F'_Z(d^2) = 2d f_Z(d^2). \tag{8}$$

C. Distance Evaluation

With coordinate distributions and the four-step approach described above, now we can evaluate the distance distribution for the three cases described in Section III-A.

1) Distance Distribution within a Unit Square: The distance distribution inside a single square is relatively simple. Mathai has already done impressive work in geometrical probability [22]. By modifying his equation (2.4.9), we can get the distance distribution of two random points, e.g., A and B in Fig. 2, as $f_{D_1}(d) =$

$$\begin{cases} 2d(\pi - 4d + d^2) & 0 \leq d \leq 1 \\ 2d[2\sin^{-1}(1/d) - 2\sin^{-1}\sqrt{1-1/d^2} & \\ \quad + 4\sqrt{d^2-1} - d^2 - 2] & 1 \leq d \leq \sqrt{2} \\ 0 & \text{otherwise} \end{cases}. \tag{9}$$

Figure 3 shows the probability density function of D_1, which is very different from the truncated normal distribution. Nevertheless, the curve of $f_{D_1}(d)$ can be very closely approximated by a polynomial fit [23], which is also plotted in the figure. Their subtle difference is shown in the zoom-in window. The degree-10 polynomial used for the approximation is

$$\begin{aligned} \widetilde{f}_{D_1}(d) = {} & 0.2802d^{10} - 2.0964d^9 + 2.2349d^8 \\ & + 24.3629d^7 - 106.8231d^6 + 194.4928d^5 \\ & - 182.8093d^4 + 91.8223d^3 - 29.3663d^2 \\ & + 8.2843d - 0.0402 \end{aligned}. \tag{10}$$

The norm of the residuals for the poly-fitting is 0.0749.

2) Distance Distribution between Two Diagonal Neighbor Squares: Although Mathai gave a generic formulation of the random node distance distribution in [22], the solution is not given and cannot be derived due to the different scenarios involved. Thus, in this section, we follow the four-step approach described above and derive the closed-form distance distribution for the nodes in diagonal neighbor grids, such as P and Q in Fig. 2.

First, given $f_{X_1}(x) = H(x) - H(x-1)$, $f_{X_2}(x) = H(x+1) - H(x)$ and $V = X_1 - X_2$, we can get

$$f_V(v) = \begin{cases} v & 0 \leq v \leq 1 \\ 2 - v & 1 \leq v \leq 2 \\ 0 & \text{otherwise} \end{cases}. \tag{11}$$

Second, given (11), we can simplify (6) into $f_S(s) = f_V(\sqrt{s})/(2\sqrt{s})$, and get

$$f_S(s) = \begin{cases} 1/2 & 0 \leq s \leq 1 \\ 1/\sqrt{s} - 1/2 & 1 \leq s \leq 4 \\ 0 & \text{otherwise} \end{cases}. \tag{12}$$

Third, by applying convolution on (12), $f_Z(z)$ for $S_X + S_Y$ is obtained as follows:

$$f_Z(z) = \begin{cases} z/4 & 0 \leq z \leq 1 \\ 2\sqrt{z} - 3z/4 - 1 & 1 \leq z \leq 2 \\ 2\sin^{-1}(1-2/z) - 4\sqrt{z-1} & \\ \quad + z/4 + 2\sqrt{z} + 1 & 2 \leq z \leq 4 \\ 2\sin^{-1}(1-2/z) - 4\sqrt{z-1} & \\ \quad + 3z/4 + 3 & 4 \leq z \leq 5 \\ 2\sin^{-1}(8/z-1) + 2\sqrt{z-4} & \\ \quad - z/4 - 2 & 5 \leq z \leq 8 \\ 0 & \text{otherwise} \end{cases}. \tag{13}$$

Finally, the probability density function of the diagonal distance distribution can be expressed as $f_{D_D}(d) =$

$$\begin{cases} 2d(d^2/4) & 0 \leq d \leq 1 \\ 2d(2d - 3d^2/4 - 1) & 1 \leq d \leq \sqrt{2} \\ 2d[2\sin^{-1}(1-2/d^2) - 4\sqrt{d^2-1} & \\ \quad + d^2/4 + 2d + 1] & \sqrt{2} \leq d \leq 2 \\ 2d[2\sin^{-1}(1-2/d^2) - 4\sqrt{d^2-1} & \\ \quad + 3d^2/4 + 3] & 2 \leq d \leq \sqrt{5} \\ 2d[2\sin^{-1}(8/d^2-1) + 2\sqrt{d^2-4} & \\ \quad - d^2/4 - 2] & \sqrt{5} \leq d \leq \sqrt{8} \\ 0 & \text{otherwise} \end{cases}. \tag{14}$$

Figure 4 shows all the intermediate results ($f_V(v)$, $f_S(s)$ and $f_Z(z)$) from the above four steps, and the final probability density function ($f_{D_D}(d)$). With a unit grid size, the distance of two random nodes in diagonal neighbor grids will be in the range of $[0, \sqrt{8}]$. This figure also shows a clear difference of the distance density function from the truncated normal distribution, but a polynomial function can have almost perfect

This full text paper was peer reviewed at the direction of IEEE Communications Society subject matter experts for publication in the IEEE INFOCOM 2010 proceedings
This paper was presented as part of the main Technical Program at IEEE INFOCOM 2010.

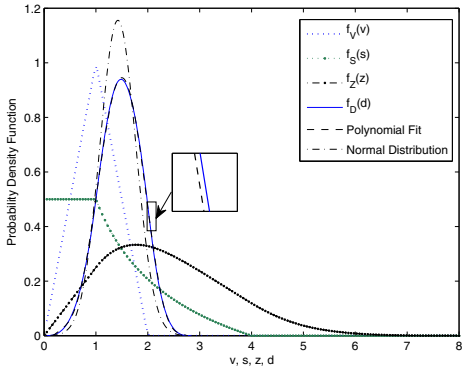

Fig. 4. Distance Distribution between Two Diagonal Neighbor Squares.

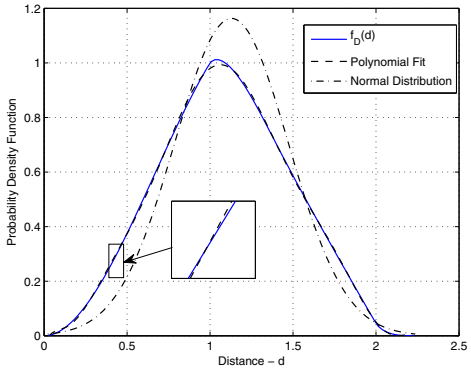

Fig. 5. Distance Distribution between Two Parallel Neighbor Squares.

match to the density function (with the difference shown in the zoom-in window). The degree-9 polynomial function, with the norm of residuals of 0.0563 with regard to the fitting, is

$$\begin{aligned}\widetilde{f}_{D_{\mathrm{D}}}(d) = {} & 0.0261d^9 - 0.1917d^8 + 0.0505d^7 \\ & + 3.1761d^6 - 11.1185d^5 + 15.4778d^4 \\ & - 9.5993d^3 + 3.0255d^2 - 0.3519d + 0.0095\end{aligned} \quad . \tag{15}$$

3) Distance Distribution between Two Parallel Neighbor Squares: Following the same approach, we can obtain the distance distribution for the case of parallel neighbor grids, such as R and S in Fig. 2. In this case, the distance range will be $[0, \sqrt{5}]$, and the parallel distance distribution is $f_{D_{\mathrm{P}}}(d) =$

$$\begin{cases} 2d(d - d^2/2) & 0 \le d \le 1 \\ 2d[\sin^{-1}(2\sqrt{d^2-1}/d^2) - 2\sqrt{d^2-1} & \\ \quad + d^2 - 2d + 3/2] & 1 \le d \le \sqrt{2} \\ 2d[\sin^{-1}(2\sqrt{d^2-1}/d^2) - 2\sqrt{d^2-1} & \\ \quad - 2d - 1/2] & \sqrt{2} \le d \le 2 \\ 2d[2\sin^{-1}(8/d^2-1) + 2\sqrt{d^2-1} & \\ \quad - \sin^{-1}(1 - 2/d^2) + \sqrt{d^2-4} & \\ \quad - d^2/2 - 5/2] & 2 \le d \le \sqrt{5} \\ 0 & \text{otherwise} \end{cases} \quad . \tag{16}$$

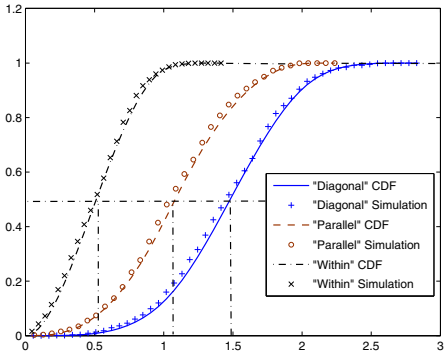

Fig. 6. Numerical and Simulation Results For Distance Distributions.

The probability density function $f_{D_{\mathrm{P}}}(d)$ is shown in Fig. 5. This curve is also different from the truncated normal distribution, but a polynomial function can match the distance distribution pretty well. The degree-11 polynomial, with the norm of residuals of 0.0697 with regard to the fitting, is

$$\begin{aligned}\widetilde{f}_{D_{\mathrm{P}}}(d) = {} & 0.0013d^{11} - 0.0184d^{10} + 0.1125d^9 \\ & - 0.3822^8 + 0.7936d^7 - 1.0403d^6 + 0.8604d^5 \\ & - 0.4373d^4 + 0.1281d^3 - 0.0179d^2 + 0.0013d\end{aligned} \quad . \tag{17}$$

Thus through a flexible formulation, we have obtained the closed-form solutions for all the three distance distribution cases in grid-based wireless sensor networks. In addition, we also got their polynomial approximation functions.

IV. Performance Evaluation

In this section, we first verify the distance distributions obtained in the previous section by simulation, and then we evaluate the energy consumption in one hop and over the entire network, and compare the approach using distance distributions and that using the average distance.

A. Distance Verification

For verification, we generated $1,000$ pairs of random points in the three cases defined in Section III-A: within the same unit grid, in the diagonal or parallel unit neighbor grids. We calculated their distance distributions according to the piecewise functions derived in the last section. As shown in Fig. 6, the simulation results match the cumulative distribution functions quite well in all three cases, with only slight deviation. This validates the accuracy of our models and derivation.

Although the piecewise functions are very accurate, using them directly for energy evaluation would not be convenient. However, the truncated normal distribution does not fit these functions well. According to Fig. 3–5, we therefore use the high-degree polynomial functions through Least Squares Fitting [23], i.e., $\widetilde{f}_{D_{\mathrm{I}}}(x)$, $\widetilde{f}_{D_{\mathrm{D}}}(x)$ and $\widetilde{f}_{D_{\mathrm{P}}}(x)$, to approximate the distribution functions, which will make the integral operation for energy calculation in the next section easier to handle.

This full text paper was peer reviewed at the direction of IEEE Communications Society subject matter experts for publication in the IEEE INFOCOM 2010 proceedings
This paper was presented as part of the main Technical Program at IEEE INFOCOM 2010.

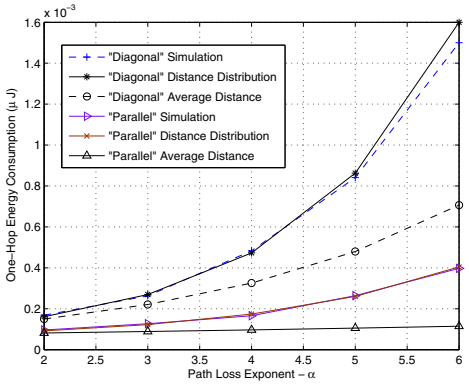

Fig. 7. One-Hop Energy Consumption with Unit Grids.

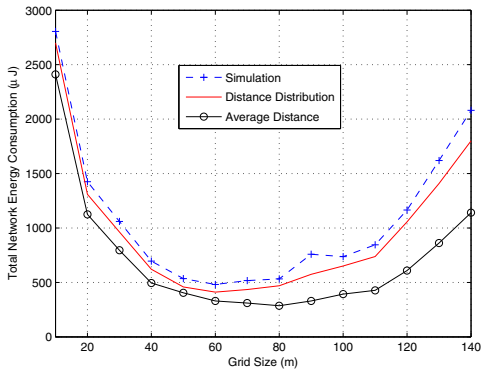

Fig. 8. Total Network Energy Consumption with Diagonal-First Routing.

B. One-Hop Energy Consumption

As motioned in Section II, both Diagonal-First Routing and Manhattan Walk rely on the one-hop neighbor information. Here we simulate the energy consumption between CHs in two neighbor grids. Note that we used the unit square grid for distance distribution formulation and calculation, since the distance can be easily scaled with the grid size. For example, the distance can be scaled to the size of either Manhattan Walk (i.e., $s \leq r/\sqrt{5}$) or Diagonal-First grids (i.e., $s' \leq r/\sqrt{8}$), for a given maximum transmission range r.

According to [5], the energy consumed by the radio transmitter can be formulated as

$$E_{\text{Tx}} = k\epsilon \int x^{\alpha} f_D(x) dx, \tag{18}$$

where k is the data transmission rate, ϵ is a constant related to the environment, and α is the path loss exponent with typical values from 2 to 6. The exact form of $f_D(x)$ is in (14) or (16), but we can use (15) or (17) to avoid the complicated piecewise calculation. Even though (18) assumes a perfect power control, the result can provide a performance bound, and our distance distribution models can be used with other energy models.

The simulation again uses $1,000$ pairs of random points in diagonal or parallel unit grids. As shown in Fig. 7, the energy consumption per bit is in the order of 10^{-3} μJ due to the unit grid size. For both diagonal and parallel grids, if the average distance is used for energy calculation, the error will increase exponentially when the path loss exponent α becomes larger. This indicates the importance of using distance distributions, instead of the average distance, to calculate energy consumption in grid-based clustering.

C. Network Energy Optimization

In order to see the impact of the average distance and distance distribution approach on the final results of network energy optimization, we simulate a wireless sensor network for an area of 200×200 m^2 and with $1,000$ sensor nodes. Due to the page limit, we only present the results for Diagonal-First routing, which is more energy efficient than Manhattan Walk according to our previous work [4].

1) Simulation Setup: In the simulation, both free-space propagation model and multi-path fading model were used. According to [3], if the transmitter-receiver distance is less than a certain cross-over distance d_c, then the Friis free-space model is used; otherwise, the two-ray ground propagation model will be applied instead. d_c is defined as

$$d_c = 4\pi\sqrt{L} h_r h_t / \lambda, \tag{19}$$

where $L \geq 1$ is the system loss factor, h_r and h_t are the height of the receiver and transmitter antenna, respectively, and λ is the wavelength of the carrier signal. Then the energy consumption between the transceivers with distance d will be

$$E_{\text{Tx}} = \begin{cases} k\epsilon_{\text{Friis}} d^2 & d \leq d_c \\ k\epsilon_{\text{two-ray}} d^4 & d \geq d_c \end{cases}. \tag{20}$$

[3] defines how to calculate the coefficients ϵ_{Friis} and $\epsilon_{\text{two-ray}}$. In our simulation, we used the following parameters: $h_t = h_r = 0.6$ m, no system loss ($L = 1$), 2.4 GHz radio frequency[2], and $\lambda = \frac{3\times10^8}{2.4\times10^9} = 0.125$ m. Plugging these numbers into (19), $d_c = 36.2$ m. The corresponding coefficients are $\epsilon_{\text{Friis}} = 0.69$ $pJ/bit/m^2$ and $\epsilon_{\text{two-ray}} = 0.051$ $pJ/bit/m^4$, respectively. The energy consumed per bit in the transceiver electronics is $E_{\text{elec}} = 50$ nJ/bit.

2) Simulation Results: In Fig. 8, the simulation and distribution analysis results of the average energy consumption to bring a bit to the sink match with each other closely, when compared with the model using the average distance. The deviation becomes larger for the average distance case when the grid size increases, as the energy consumption will follow the two-ray ground mode with a path loss exponent of 4.

There also exists an optimal grid size, at which the total energy is minimized. This is consistent with the result in [4]. The optimal value in the distribution analysis and simulation, however, is very different from that achieved in the average distance model. This again confirms that the calculation of the distance distribution models capture the reality very well,

[2]According to IEEE 802.15.4 specification, ZigBee operates in the Industrial, Scientific and Medical (ISM) radio bands: 868 MHz in Europe, 915 MHz in the USA and Australia, and 2.4 GHz in most other jurisdictions worldwide. Our calculation can be easily applied to other frequency bands.

This full text paper was peer reviewed at the direction of IEEE Communications Society subject matter experts for publication in the IEEE INFOCOM 2010 proceedings
This paper was presented as part of the main Technical Program at IEEE INFOCOM 2010.

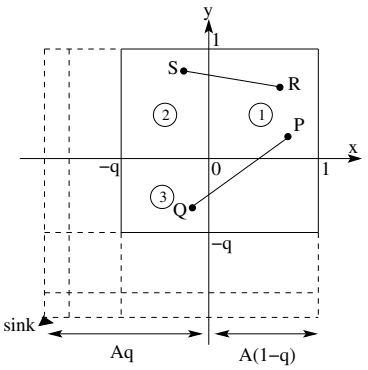

Fig. 9. Nonuniform Griding with Size Ratio q.

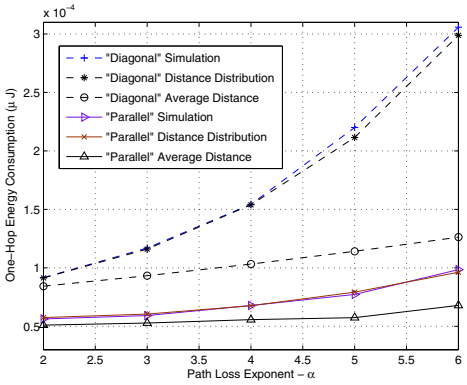

Fig. 10. One-Hop Energy Consumption with Variable-Size Grids.

therefore it is worthwhile to pay the extra effort for better accuracy, especially when such effort only happens at the network planning stage and can be amortized over a much longer network lifetime if an optimal grid size is used.

V. Performance Improvement

As mentioned before, the data traffic in sensor networks often follows a many-to-one pattern. The regions close to the sink, therefore, are more likely to become the hot-spot crowded with data transmission. The uniform grid structure discussed in the previous sections gives us a baseline, which we can improve further and show how variable-size grids can affect the network energy consumption. Here we give numerical and simulation results showing the optimality of the grid size ratio. A theoretical proof of the optimality is our ongoing work.

A. Variable-size Griding

Also pointed out in [4], variable-size griding is advantageous in smoothing out the energy consumption in the entire sensing field. Grids close to the sink will have a smaller grid size, and thus have a shorter transmission distance when compared with the grids that are farther away. Although having a larger amount of data, less energy per unit data is needed for the transmission between these close-to-sink grids, which alleviates the impact of the uneven traffic volume.

Suppose in Fig. 9, the sink node is located at the lower left corner of a field with size $A \times A$. We divide the field recursively with size ratio q, a value between 0 and 1. Sensors can use either Diagonal-First routing or Manhattan Walk to forward data to the sink node. Notice that if the sink is located at an arbitrary position in the field, this division method can be repeated in four different quadrants with the sink node at the corner. The nonuniform griding with a fixed ratio q is a special case of the variable-size griding, which we use in this paper for illustration purpose.

B. Distance Distribution With Nonuniform Griding

Without loss of generality, we have the coordination system as shown in Fig. 9 for nonuniform grids. Here we normalize the size of grid ① to a unit square, then grid ② has size $q \times 1$, and grid ③ has size $q \times q$, where $0 < q < 1$. For P and Q in grid ①, their coordinate distributions should be reformulated with the Heaviside Step Function $H(x)$ as

$$\begin{cases} f_{X_1}(x) = f_{Y_1}(x) = H(x) - H(x-1) \\ f_{X_2}(x) = f_{Y_2}(x) = [H(x+q) - H(x)]/q \end{cases}, \tag{21}$$

i.e., $X_1, Y_1 \sim U[0,1]$ and $X_2, Y_2 \sim U[-q, 0]$.

Then we can get the node distance distribution in the diagonal nonuniform case following the same four-step derivation in Section III. Depending on the value of q, the convolution in Section III-B1 will have completely different results. The probability density function $f_{D'_{\mathrm{D}}}(d)$, in the case where $(\sqrt{2}-1) \le q \le 1/\sqrt{2}$, is listed as (22) in Appendix. Other ranges of q are $0 \le q \le (\sqrt{3}-1)/2$, $(\sqrt{3}-1)/2 \le q \le (\sqrt{2}-1)$ and $1/\sqrt{2} \le q \le 1$, and can be derived accordingly.

For nodes in parallel grids, e.g., R and S in Fig. 9, the distance distributions can also be calculated. $f_{D'_{\mathrm{P}}}(d)$ in the case where $(\sqrt{2}-1) \le q \le 1$ is listed as (23) in Appendix.

C. Energy Efficiency with Nonuniform Griding

Figure 10 shows both the numerical and simulation results in the case of one-hop energy consumption for grids in Diagonal-First routing and Manhattan Walk, with grid size ratio $q = 0.5$. Distance distribution models here perform better than the average distance model as well. Notice that the energy scale in this figure is even smaller than that in Fig. 7, since the size of one grid is scaled with ratio q.

Figure 11 shows the case where in a 200×200 m^2 network, using fixed grid size vs. nonuniform grid size for Diagonal-First routing. The total number of grids are chosen to be 4×4 since 50 m is the optimal grid size in Fig. 8. Here the energy consumption per grid is sorted in the increasing order for each grid in the network. Compared with $q = 0.4$ and $q = 0.5$, it is obvious that nonuniform griding with a proper grid size ratio can reduce the maximum energy consumption, thus balancing the overall energy distribution. According to the average value in the figure, nonuniform griding also has the potential to reduce the average energy consumption.

Figure 12 shows the simulation results of the total network energy consumption with different values of q. For Diagonal-First routing, when q is within the range of 0.3–0.6, the total

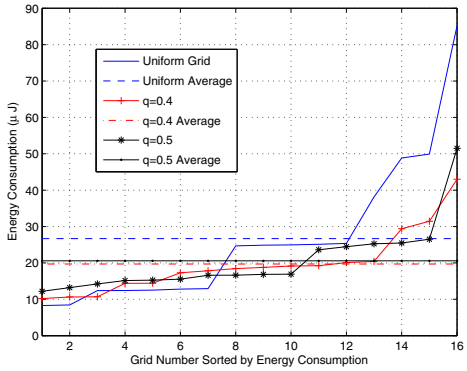

Fig. 11. Per-Grid Energy Consumption with Variable-Size Grids.

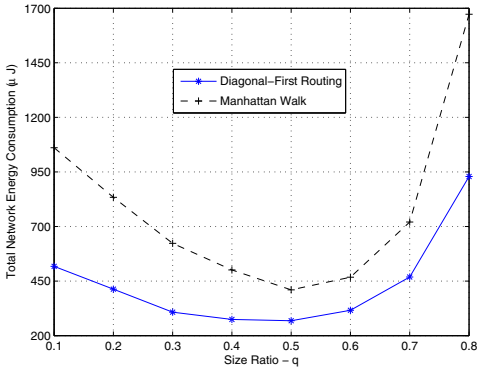

Fig. 12. Total Network Energy Consumption with Variable-Size Grids.

energy is reduced by nearly 40% compared to Fig. 8. When q becomes larger, however, nonuniform grid size no longer improves network energy efficiency since the nodes close to the sink have a longer transmission range. In the figure we can also tell Manhattan Walk is more sensitive to the grid size ratio than Diagonal-First routing.

VI. Further Discussion and Conclusions

In this paper, we first proposed energy consumption models with distance distributions for grid-based wireless sensor networks. Previous work in this area mainly used the average distances within a grid and between neighbor grids, which we found is not accurate and can largely underestimate the actual value. Due to the popularity of grid-based clustering schemes, we believe that it is worthwhile to develop more accurate energy consumption models. Using distance distributions rather than the average distance is an important step towards the goal.

In addition, we also illustrated how to use the distance distribution models in a computation-efficient manner through polynomial fitting. With the polynomial representation, distance-dominated energy consumption can be easily derived and calculated, in order to minimize overall energy consumption and prolong network lifetime for different griding schemes. We further used the distance distribution models to investigate the impact of variable-size griding with a fixed grid size ratio (i.e., nonuniform griding), and the performance evaluation showed the potential of the new scheme and the capability of the distance models developed in this paper.

Due to the simplicity and feasibility of grid-based clustering schemes in the real world, the pursuit to further improve its energy efficiency has been an active research topic, and we expect to continue investigating other energy-saving opportunities, such as opportunistic forwarding where in some cases the node can communicate not only with the nodes in their immediate neighbor grids, but also the nodes further away towards the destination, which reduces the number of hops (or transmissions) needed to reach the destination.

References

[1] K. Akkaya, M. Younis, "A survey on routing protocols for wireless sensor networks," *Ad Hoc Networks,* vol. 3, no. 3, pp. 325–349, May 2005.
[2] I. Demirkol, C. Ersoy, F. Alagoz, "MAC protocols for wireless sensor networks: a survey," *IEEE Comm Magazine,* 44(4):115–121, April 2006.
[3] W. R. Heinzelman, A. Chandrakasan, and H. Balakrishnan, "Energy-efficient communication protocol for wireless microsensor networks," *Hawaii International Conference on System Sciences (HICSS)*, 2000.
[4] Y. Zhuang, J. Pan and G. Wu, "Energy-optimal grid-based clustering in wireless microsensor networks," *IEEE ICDCS Workshop on Wireless Ad hoc and Sensor Networking (WWASN)*, 2009.
[5] W. B. Heinzelman, A. P. Chandrakasan, and H. Balakrishnan, "An application-specific protocol architecture for wireless microsensor networks," *Wireless Communications, IEEE Trans on*, 1(4):660–670, 2002.
[6] W. Choi, P. Shah and S.K. Das,"A framework for energy-saving data gathering using two-phase clustering in wireless sensor networks," *Mobile and Ubiquitous Systems: Networking and Services, 2004*.
[7] P. Cheng, C.-N. Chuah, and X. Liu, "Energy-aware node placement in wireless sensor networks," *IEEE GLOBECOM*, 2004.
[8] Q. Gao, K. J. Blow, D. J. Holding, I. Marshall, and X. H. Peng, "Radio Range Adjustment for Energy Efficient Wireless Sensor Networks," *Ad-Hoc Networks*, pp. 75–82, January 2006.
[9] R. Akl and U. Sawant, "Grid-based coordinated routing in wireless sensor networks," *IEEE CCNC*, 2007.
[10] R. Vidhyapriya and P. T. Vanathi, "Energy efficient grid-based routing in wireless sensor networks," *International Journal of Intelligent Computing and Cybernetics*, vol. 1, no. 2, pp. 301–318, Jan. 2008.
[11] V. Mhatre, C. Rosenberg, D. Kofman, R. Mazumdar and N. Shroff, "A minimum cost heterogeneous sensor network with a lifetime constraint," *IEEE Trans on Mobile Computing*, vol. 4, no. 1, pp. 4–15, 2005.
[12] O. Younis and S. Fahmy, "Distributed clustering in ad-hoc sensor networks: A hybrid, energy-efficient approach," *IEEE INFOCOM*, 2004.
[13] L. Lazos and R. Poovendran, "Serloc: Robust localization for wireless sensor networks," *ACM Trans. Sen. Netw.*, vol. 1, no. 1, pp. 73–100, 2005.
[14] Y. Xu, J. Heidemann, and D. Estrin, "Geography-informed energy conservation for ad hoc routing," *ACM MobiCom*, 2001.
[15] S. Phoha, T.F. La Porta, and C. Griffin, "Sensor Network Operations," Wiley-IEEE Press, 2006.
[16] KH. Liu, L. Cai, and X. Shen, "Exclusive-region based scheduling algorithms for UWB WPAN," *IEEE Trans on Wireless Comm*, 2008.
[17] S. Soro and W. Heinzelman, "Prolonging the lifetime of wireless sensor networks via unequal clustering," *IEEE IPDPS,* 2005.
[18] M. Ye, C. Li, G. Chen and J. Wu, "EECS: an energy efficient clustering scheme in wireless sensor networks," *International Performance, Computing, and Communications Conference (IPCCC)*, 2005.
[19] A. Egorova-Forster, and A. Murphy, "Exploring Non Uniform Quality of Service for Extending WSN Lifetime," *International Conference on Pervasive Computing and Communications Workshops*, 2007.
[20] W. Dai, L. Liu, and T.D. Tran, "Adaptive block-based image coding with pre-/post-filtering," *Data Compression Conference*, 2005.
[21] Weisstein, Eric W. "Heaviside Step Function," From MathWorld–A Wolfram Web Resource. http://mathworld.wolfram.com/HeavisideStepFunction.html
[22] A.M. Mathai, "An introduction to geometrical probability: distributed aspects with applications," Gordon and Breach Science Publishers, 1999.
[23] Weisstein, Eric W. "Least Squares Fitting," From MathWorld–A Wolfram Web Resource. http://mathworld.wolfram.com/LeastSquaresFitting.html

This full text paper was peer reviewed at the direction of IEEE Communications Society subject matter experts for publication in the IEEE INFOCOM 2010 proceedings
This paper was presented as part of the main Technical Program at IEEE INFOCOM 2010.

APPENDIX

A. Distance Distribution between Two Diagonal Neighbor Squares with Size Ratio q

The probability density function $f_{D'_{\mathrm{D}}}(d)$ of P and Q in Fig. 9, in the case where $(\sqrt{2}-1) \le q \le \frac{1}{\sqrt{2}}$, is $f_{D'_{\mathrm{D}}}(d) =$

$$
\begin{cases}
d\frac{d^2}{2q^2} & 0 \le d \le q \\
d(\frac{2d}{q} - \frac{d^2}{2q^2} - 1) & q \le d \le \sqrt{2}q \\
d\{\sin^{-1}\left(\frac{d^2-2q^2}{d^2}\right) + \frac{2}{q}\left[d - \sqrt{d^2-q^2}\right]\} & \sqrt{2}q \le d \le 1 \\
d\{\sin^{-1}\left(\frac{d^2-2q^2}{d^2}\right) + \frac{2}{q^2}\left[(1+q)d - q\sqrt{d^2-q^2}\right] - \frac{d^2}{q^2} - \frac{1}{q^2}\} & 1 \le d \le \sqrt{1+q^2} \\
d\{\frac{1}{q}\left[\sin^{-1}\left(\frac{d^2-2}{d^2}\right) + (1+q)\sin^{-1}\left(\frac{d^2-2q^2}{d^2}\right)\right] - 2\frac{\sqrt{d^2-1}}{q} + 1 & \\
\quad + 2\frac{1+q}{q^2}(d - \sqrt{d^2-q^2})\} & \sqrt{1+q^2} \le d \le \sqrt{2} \\
d\{\frac{1+q}{q^2}\left[\sin^{-1}\left(\frac{d^2-2}{d^2}\right) + q\sin^{-1}\left(\frac{d^2-2q^2}{d^2}\right)\right] + \frac{d^2}{2q^2} + \frac{1+q^2}{q^2} & \\
\quad + 2\frac{1+q}{q^2}(d - \sqrt{d^2-q^2} - \sqrt{d^2-1})\} & \sqrt{2} \le d \le (1+q) \\
d\{\frac{1+q}{q^2}\left[\sin^{-1}\left(\frac{d^2-2}{d^2}\right) + q\sin^{-1}\left(\frac{d^2-2q^2}{d^2}\right)\right] + \frac{3d^2}{2q^2} + 2\frac{1+q+q^2}{q^2} & \\
\quad - 2\frac{1+q}{q^2}(\sqrt{d^2-q^2} + \sqrt{d^2-1})\} & (1+q) \le d \le \sqrt{q^2+(1+q)^2} \\
d\{\frac{1+q}{q^2}\left[\sin^{-1}\left(\frac{d^2-2}{d^2}\right) + q\sin^{-1}\left(\frac{2(1+q)^2-d^2}{d^2}\right)\right] + \frac{d^2}{2q^2} + \frac{1}{q^2} & \\
\quad + \frac{2}{q^2}\left[q\sqrt{d^2-(1+q)^2} - (1+q)\sqrt{d^2-1}\right]\} & \sqrt{q^2+(1+q)^2} \le d \le \sqrt{1+(1+q)^2} \\
d\{\frac{(1+q)^2}{q^2}\sin^{-1}\left[\frac{2(1+q)^2-d^2}{d^2}\right] - \frac{d^2}{2q^2} & \\
\quad - \frac{1+q}{q^2}\left[(1+q) - 2\sqrt{d^2-(1+q)^2}\right]\} & \sqrt{1+(1+q)^2} \le d \le \sqrt{2}(1+q) \\
0 & \text{otherwise}
\end{cases}
\tag{22}
$$

B. Distance Distribution between Two Parallel Neighbor Squares with Size Ratio q

The probability density function $f_{D'_{\mathrm{P}}}(d)$ of R and S in Fig. 9, where $(\sqrt{2}-1) \le q \le 1$, is $f_{D'_{\mathrm{P}}}(d) =$

$$
\begin{cases}
d(\frac{2d}{q} - \frac{d^2}{q}) & 0 \le d \le q \\
d[\frac{\pi}{2} - \sin^{-1}\left(\frac{2q^2-d^2}{d^2}\right) + 2\frac{1-q}{q}d - 2\frac{\sqrt{d^2-q^2}}{q} + q] & q \le d \le 1 \\
d\{\frac{1+q}{2q}\pi - \frac{1}{q}\left[\sin^{-1}\left(\frac{2-d^2}{d^2}\right) + q\sin^{-1}\left(\frac{2q^2-d^2}{d^2}\right)\right] + \frac{2d^2}{q} & \\
\quad - 2\frac{\sqrt{d^2-q^2}}{q} - 2\frac{\sqrt{d^2-1}}{q} - \frac{2(1+q)}{q}d + \frac{q^2+2}{q}\} & 1 \le d \le \sqrt{1+q^2} \\
d[\frac{1+q}{2q}\pi + \frac{q-1}{q}\sin^{-1}\left(\frac{2-d^2}{d^2}\right) + \frac{d^2}{q} - \frac{2(1+q)}{q}d + \frac{2(q-1)}{q}\sqrt{d^2-1} + \frac{1}{q}] & \sqrt{1+q^2} \le d \le \sqrt{2} \\
d[\frac{1+q}{2q}\pi - \frac{1+q}{q}\sin^{-1}\left(\frac{d^2-2}{d^2}\right) + \frac{2(1+q)}{sq}\left(\sqrt{d^2-1} - d\right) - \frac{1}{q}] & \sqrt{2} \le d \le 1+q \\
d\{\frac{1+q}{q}\left[\sin^{-1}\left(\frac{2(1+q)^2-d^2}{d^2}\right) - \sin^{-1}\left(\frac{d^2-2}{d^2}\right)\right] + 2\frac{\sqrt{d^2-(1+q)^2}}{q} & \\
\quad + \frac{2(1+q)}{q}\sqrt{d^2-1} - \frac{d^2}{q} - \frac{q^2+2q+2}{q}\} & 1+q \le d \le \sqrt{(1+q)^2+1} \\
0 & \text{otherwise}
\end{cases}
\tag{23}
$$

ACKNOWLEDGMENT

This work is supported in part by the Natural Sciences and Engineering Research Council of Canada (NSERC), Canada Foundation for Innovation (CFI) and British Columbia Knowledge Development Fund (BCKDF). Yanyan Zhuang also wants to thank the support from the Ministry of Education's Key Laboratory of Computer Network and Information Integration (CNII) at the Department of Computer Science and Engineering, Southeast University, Nanjing, China.